

Article

Influence of Foreign Salts and Antiscalants on Calcium Carbonate Crystallization

Raghda Hamdi ^{1,*}  and Mohamed Mouldi Tlili ² 

¹ Department of Chemistry, College of Science and Humanities in Al-Kharj, Prince Sattam bin Abdulaziz University, Al-Kharj 11942, Saudi Arabia

² Laboratory of Desalination and Natural Water Valorisation (LADVEN), Water Researches and Technologies Center (CERTe), Techno-Park Borj Cedria, BP 273, Soliman 8020, Tunisia

* Correspondence: hamdi.raghda@gmail.com

Abstract: For more than a century, crystallization has remained a chief research topic. One of the most undesirable crystallization phenomena is the formation of calcium carbonate scale in drinking and industrial water systems. In this work, the influence of chemical additives on CaCO₃ formation—in either nucleation, crystal growth, or inhibition processes—is investigated by using the CO₂-degasification method. Chemical additives are foreign salts (MgCl₂, Na₂SO₄ and MgSO₄) to the calco-carbonic system and antiscalants (sodium polyacrylate ‘RPI’ and sodium-tripolyphosphate ‘STPP’). The results show that additives affects both crystallization kinetics and the CaCO₃ microstructure. Sulfate and magnesium ions, added separately at constant ionic strength, influence the nucleation step more than the growth of the formed crystallites. Added simultaneously, their effect was accentuated on both nucleation and the growth of CaCO₃. Furthermore, antiscalants RPI and STPP affect the crystallization process by greatly delaying the precipitation time and largely increasing the supersaturation coefficient. It was also shown that the calco-carbonic system with additives prefers the heterogeneous nucleation to the homogeneous one. X-ray diffraction patterns show that additives promote the formation of a new crystal polymorph of calcium carbonate as aragonite, in addition to the initial polymorphs formed as calcite and vaterite.

Keywords: calcium carbonate; foreign salts; antiscalants; crystallization



Citation: Hamdi, R.; Tlili, M.M.

Influence of Foreign Salts and Antiscalants on Calcium Carbonate Crystallization. *Crystals* **2023**, *13*, 516. <https://doi.org/10.3390/cryst13030516>

Academic Editor: José L. Arias

Received: 28 February 2023

Revised: 13 March 2023

Accepted: 15 March 2023

Published: 17 March 2023



Copyright: © 2023 by the authors. Licensee MDPI, Basel, Switzerland. This article is an open access article distributed under the terms and conditions of the Creative Commons Attribution (CC BY) license (<https://creativecommons.org/licenses/by/4.0/>).

1. Introduction

Crystallization in the calco-carbonic system CaCO₃-CO₂-H₂O and the parameters that significantly control the polymorph’s formation have been studied for more than a century by several researchers in different scientific disciplines ranging from industrial crystallization [1,2] to biomineralization [3–5].

Calcium carbonate exists in three crystalline forms, which are calcite, aragonite and vaterite, in the order of stability at earth surface conditions. These crystalline phases have different crystal structures and morphologies. Calcite, aragonite and vaterite crystals have rhombohedral, orthorhombic, and hexagonal structures, respectively. In addition, crystalline monohydrocalcite (CaCO₃.H₂O) and ikaite (CaCO₃.6H₂O) are known. The observation of an intermediated or transient amorphous phase (amorphous calcium carbonate ACC) has also been reported [6–9]. In accordance with the Ostwald’s step rule [10], the transformation of the unstable phase (ACC) to a metastable phase (vaterite or aragonite) is followed by the formation of the more stable phase (calcite) through dissolution–crystallization reactions of various degrees of complexity.

The nucleation and growth of these forms are generally related to kinetic and thermodynamic factors such as the degree of supersaturation, solvent, organic, and inorganic additives. CaCO₃ crystallization is intensely affected by the presence of such additives, which delay or inhibit nucleation and growth, and change the polymorph morphology [11–13].

The additives' impact is detected in the nucleation and growth steps [14–18]. In the current work, the effect of different types of chemical additives such as magnesium, sulfate, and antiscalants on the CaCO₃ crystallization process was studied.

The presence of dissolved ions, for instance magnesium and sulfate, is supposed to produce modification in the kinetic and the driving force of calcium carbonate precipitation [19,20]. They have long been considered as additives in calcium carbonates, usually known to affect calcite growth and dissolution. Magnesium ions have a significant role in the formation and transformation phases of CaCO₃ crystals. They inhibit calcite formation [18,21] by decelerating its growth rate [22] and favoring the appearance of aragonite [23] and monohydrocalcite [24], which are less stable phases. They extend the duration of the amorphous phase life [25], and determine the polymorph formation. Magnesium interacts directly with calcium carbonate crystals and affects their morphologies [26]. The presence of magnesium and sulfate, separately and together, modifies the shape of the calcite crystal [27]. Sulfate affects the nucleation even at lower concentrations, by suppressing the formation of CaCO₃ crystals and modifying their morphology [28]. It reduces the crystallization rate and favors the formation of the aragonite form [29].

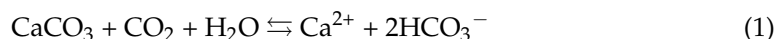
The addition of antiscalants, also known as chemical inhibitors, is an effective method to inhibit the formation of scale [30]. Indeed, antiscalants delay calcium carbonate crystallization through growth sites blocking [31]. They have three mechanisms of action, which are dispersion, chelation, and crystal modification, consisting of the distortion of the crystal to become irregular and less adhesive, thus inhibiting crystal growth at calcite surfaces [32]. The polymer adsorption on the crystal growing surface suppresses the growth rate and displaces the precipitation mode from the most thermodynamic stable phase (calcite) to the metastable phases (aragonite and vaterite) [33]. The addition of the inhibitor resulted in (i) an important inhibition of crystallization, and (ii) a porous or an unconsolidated consistency of precipitates [34]. Therefore, the incorporation of the chemical additives in the structure of the crystal phase form modified its thermodynamic properties.

The present paper aims to improve our understanding of the effect of chemical additives on the CaCO₃ crystallization. The changes induced in the kinetic, thermodynamic, and morphology of CaCO₃ phases formed after the use of diverse types of chemical additives will be evaluated to explore the complex behaviors of the crystallization described in the calco-carbonic system. Consequently, the experimental process for CaCO₃ crystallization based on the fast controlled precipitation (FCP) method [35,36] will be used. The chemical additives employed are three foreign salt (MgCl₂, Na₂SO₄, and MgSO₄) and two antiscalants (sodium polyacrylate and sodium-tripolyphosphate).

2. Experimental Section

2.1. Solution Preparation

The pure calco-carbonic water (PCCW) was obtained by the dissolution of reagent grade calcium carbonate solid in distilled water under CO₂ bubbling, as follows:



The initial pH value was fixed at 5.9, which corresponds to a supersaturation coefficient equal to 0.25 (calculated using Equation (2)) to maintain the solution undersaturated.

The degree of supersaturation (Ω) with respect to calcite, the most CaCO₃ stable form, is defined as follows:

$$\Omega_{\text{CaCO}_3} = \frac{[\text{Ca}^{2+}] \cdot [\text{CO}_3^{2-}] \cdot \gamma_{\text{Ca}^{2+}} \cdot \gamma_{\text{CO}_3^{2-}}}{K_s(\text{calcite})} \quad (2)$$

where $[i]$, γ_i and $K_s(\text{calcite})$ are the ions' concentrations, the activity coefficients and the solubility product of calcite, respectively.

All the additives used were introduced to the PCCW before the precipitation test. Studied foreign salts (MgCl₂, Na₂SO₄, and MgSO₄) quantities were calculated according

to the solution ionic strengths (IS) of about 0.012 (IS₀), 0.024 (IS₁) and 0.036 mol L⁻¹ (IS₂). The antiscalants used were organic sodium salt of polyacrylate (C₃H₃NaO₂)_n and inorganic sodium tripolyphosphate (Na₅P₃O₁₀), thereafter called, respectively, RPI and STPP. The corresponding quantities used are small and do not affect the ionic strength and the resistivity.

2.2. Fast Controlled Precipitation Set Up

The experimental set up of the fast controlled precipitation (FCP) method was presented in Figure 1. Thermostatic water bath was used to maintain the temperature of the FCP test at 30 °C. A 0.5 L volume of pure calco-carbonic water (PCCW) was filled in a polytetrafluoroethylene (PTFE) cell and was stirred at 800 rpm. The solution pH and resistivity values were constantly measured each 5 min, using a pH meter (Hanna HI 110, Hanna Instruments, Woonsocket, RI, USA) and a conductivity meter (Meter Lab CDM210, Radiometer Analytical's, Villeurbanne, France). The measuring electrode positions in the round bottom cell were well controlled. The calcium ion concentration was measured using EDTA complexometric titration.

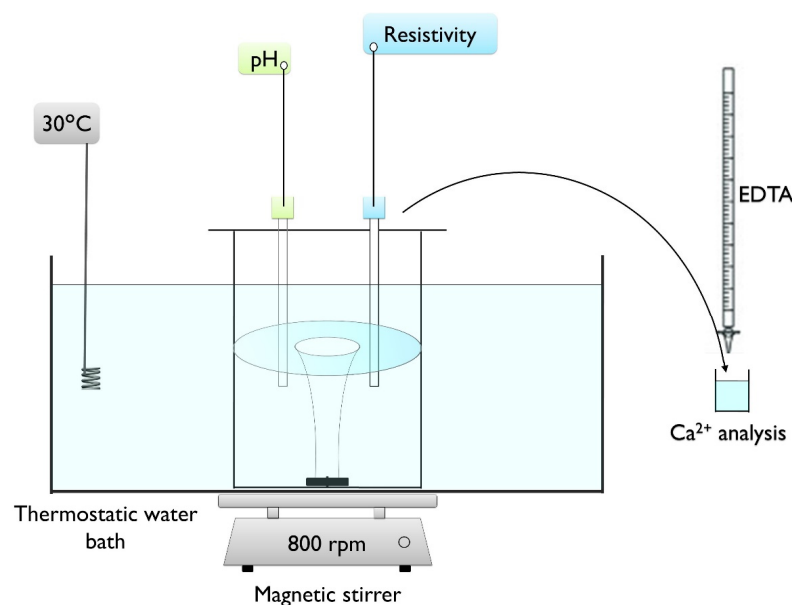


Figure 1. Fast controlled precipitation experimental set up.

In the FCP vessel, CaCO₃ can precipitate on the cell wall and in the bulk solution. After the completion of the experiment, homogeneously formed precipitate m_b can be recuperated by filtration using cellulose nitrate membrane with 0.45 μm porosity. The amount of Ca²⁺ residual in the solution was measured, and then the total precipitated calcium carbonate m_t was calculated. The heterogeneous mass m_w deposited on the cell wall can be deduced ($m_w = m_t - m_b$), and its rate is calculated as follows:

$$\%_{\text{hete}} = \frac{m_w}{m_t} \times 100 \quad (3)$$

Figure 2 represents a model of an FCP test reporting the evolution of pH and resistivity as a function of time of PCCW throughout the crystallization procedure. The figure emphasizes the limit between three different zones of precipitation. During zone 1, the resistivity is roughly constant and pH values increase up to reach the prenucleation pH “pH_{prenuc}” at t_{prenuc} . In zone 2, the pH continues rising up with a small change in the resistivity variation speed before precipitation time “ t_{prec} ”. The medium is considered to be supersaturated, and calcium carbonate precipitation is thermodynamically possible. In zone 3, the slope of the resistivity temporal evolution diverges significantly, which highlights

the precipitation beginning. After attaining the precipitation threshold at “pH_{prec}”, the pH decreases considerably. Therefore, the precipitation is rapid and followed by a crystal growth stage.

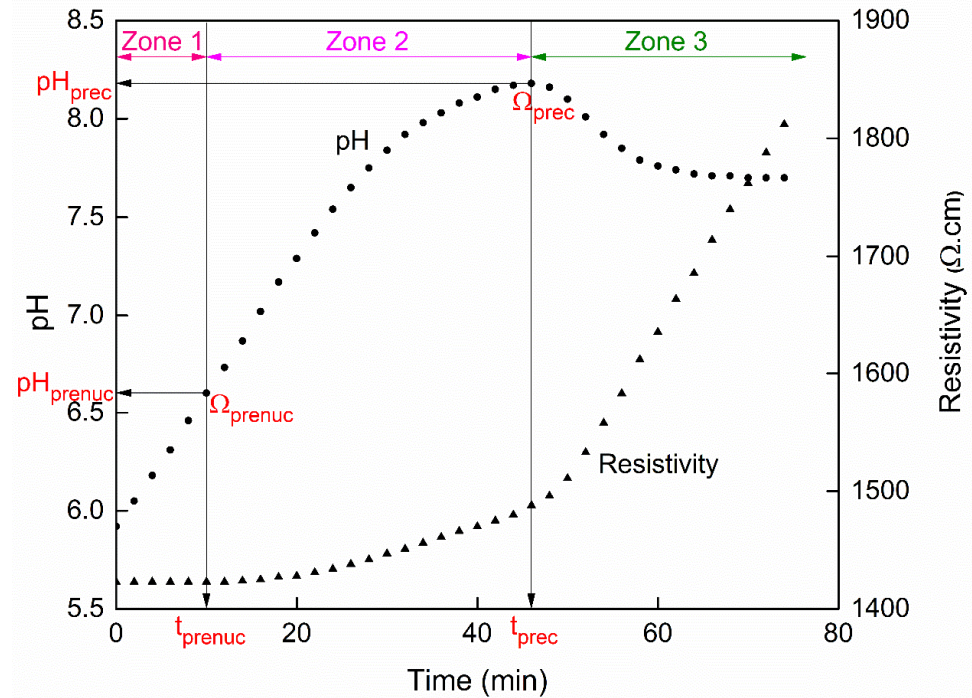


Figure 2. Temporal evolution of pH and resistivity curves of a PCCW 400 mg L⁻¹ at 30 °C, 800 rpm.

The reproducibility of the experimental measurements was verified for three FCP tests using 400 mg L⁻¹ of PCCW, as seen in Figure 3.

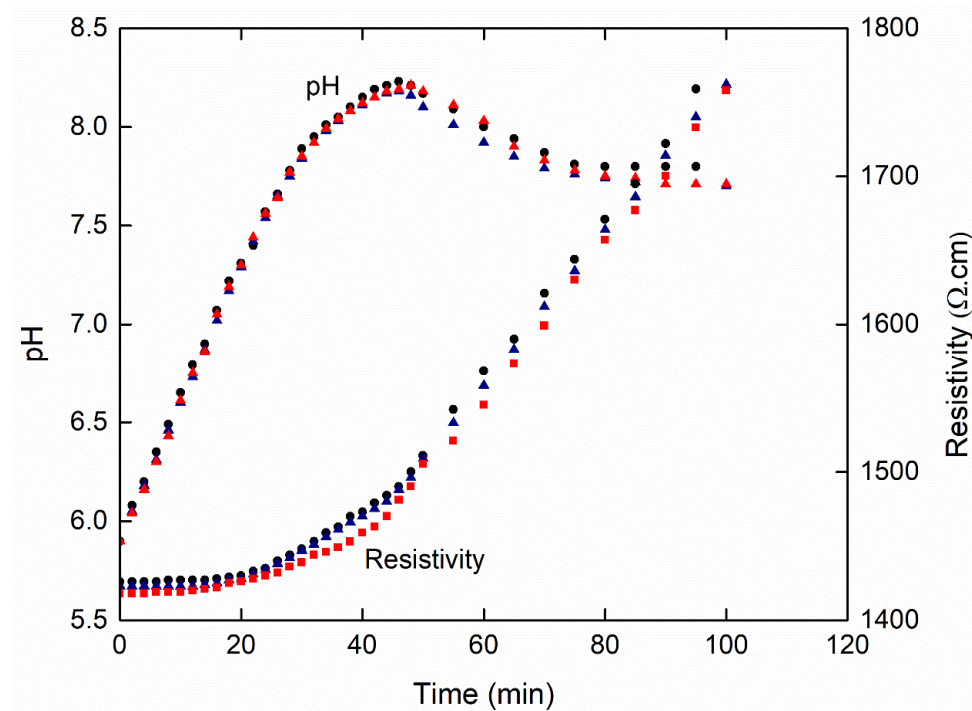


Figure 3. Reproducibility of the temporal evolution of pH and resistivity curves for three FCP tests at 30 °C, 800 rpm and PCCW 400 mg L⁻¹.

2.3. X-ray Diffraction Method for Solid Precipitate Characterization

The X-ray Diffraction (XRD) method is a very efficient and universal tool for determining the structure of crystals. At the end of each FCP test, the precipitate was recuperated by solution filtration through cellulose nitrate membrane with 0.45 μm porosity. The collected samples were dried at ambient conditions before XRD analysis. The analyses were performed using a diffractometer Philips X'PERT PRO (PANalytical, Philips, Amsterdam, The Netherlands) in step-scanning mode using Cu $K\alpha$ (1.54 \AA) radiation. The XRD patterns were chronicled in the angular range $2\theta = 10\text{--}60^\circ$, with a slight step size of $2\theta = 0.017^\circ$ and a fixed count time of 4 s. The software 'X-Pert HighScore Plus' was used to determine the XRD reflection positions. The XRD patterns of the formed precipitates were compared to the joint committee on powder diffraction standards data.

3. Results and Discussion

3.1. Effect of Initial Calcium Carbonate Concentration

The calcium carbonate concentrations vary in natural waters in a range of 100 to 600 mg L^{-1} . Examples include geothermal water (100 mg L^{-1}), tap water (200 to 400 mg L^{-1}), and saline water (600 mg L^{-1}) [37]. Therefore, three solutions with different dissolved CaCO_3 content levels (200, 400, 600 mg L^{-1}) were prepared to study the effect of initial calcium carbonate amount on the nucleation threshold. Figure 4 reports the temporal evolution of pH and $\Delta\text{Resistivity}$ curves during the FCP tests by varying the initial concentration of calcium carbonate. The main results are presented in Table 1.

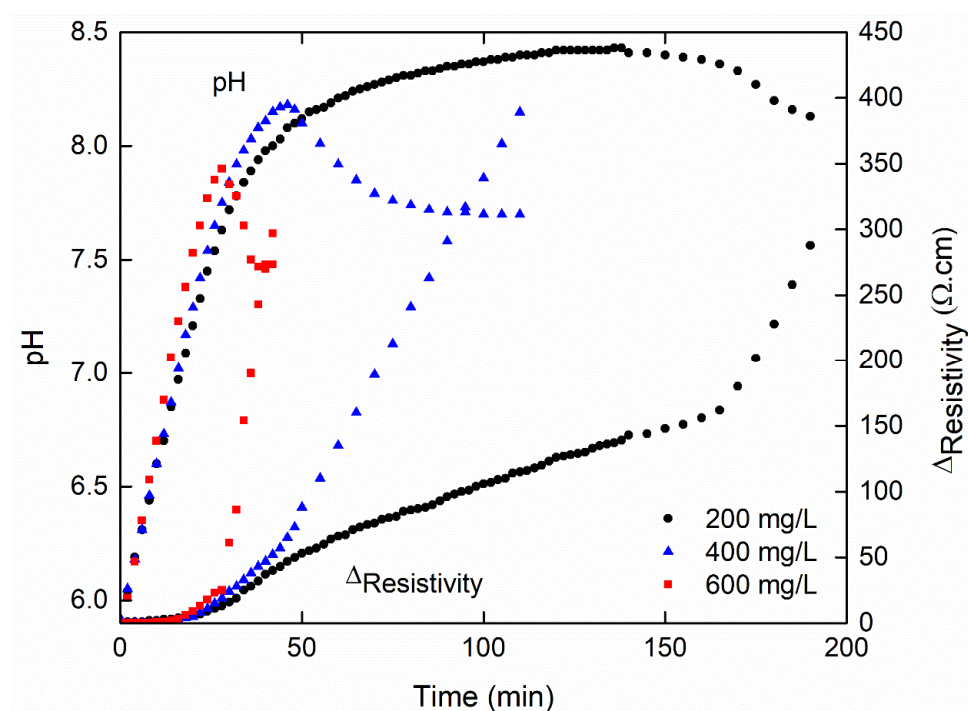


Figure 4. pH and $\Delta\text{Resistivity}$ vs. time curves by varying the initial amount of calcium carbonate.

Table 1. FCP tests results by varying the initial amount of calcium carbonate.

$[\text{CaCO}_3]_i$ (mg L^{-1})	t_{prenuc} (min)	Ω_{prenuc}	t_{prec} (min)	Ω_{prec}	Δt (min)	% _{hete}
200	18	1.1	138	24	120	56
400	12	1.7	46	48	34	45
600	8	2.0	28	51	20	34

As seen in Figure 4, the prenucleation (t_{prenuc}) and the precipitation (t_{prec}) time decrease as the CaCO_3 amount increases. Indeed, t_{prenuc} and t_{prec} are roughly divided by two and by five, respectively, as the initial concentration increases from 200 to 600 mg L^{-1} (Table 1). Ben Amor et al. [38] proved that the precipitation time was delayed from 90 to 7 min after increasing the water hardness from 20 to 50 °F by using a CO_2 degasification test. Additionally, Fathi et al. [39] found that the increase in $\text{Ca}(\text{HCO}_3)_2$ content initially dissolved from 30 to 50 °F accelerates the nucleation time from 20 to 7 min.

Thus, the nucleation step ($\Delta t = t_{\text{prec}} - t_{\text{prenuc}}$) is shorter as the initial calcium carbonate concentration increases. According to Table 1, this nucleation phase lasts 120 min for 200 mg L^{-1} and only 20 min for 600 mg L^{-1} . This can be explained by the fact that the medium saturation state is affected by the initial concentration. According to Raffaella et al. [8], the lifetime of a cluster, before the growth phase, becomes longer when the concentration decreases as a result of the reduction in collision frequency. Indeed, the variation in the solution concentration modifies the frequency of collisions between the different species present (ions, ions pairs, and clusters). Thus, the maximum size that a germ can reach varies according to the different equilibria between the association and dissociation processes.

From a thermodynamic point of view, the prenucleation threshold is attained at low Ω values less than two despite the difference in time to reach it (8 min for 600 mg L^{-1} and 18 min for 200 mg L^{-1}). However, at the precipitation threshold, the supersaturation coefficients increase from 24 to 51 and the time decreases from 138 to 28 min as the initial concentration of calcium carbonate increases from 200 mg L^{-1} to 600 mg L^{-1} , respectively.

Table 1 also reveals that the initial concentration of calcium carbonate $[\text{CaCO}_3]_i$ influences the heterogeneous precipitation rate ($\%_{\text{hete}}$) of CaCO_3 . Indeed, $\%_{\text{hete}}$ decreases from 56 to 34% as $[\text{CaCO}_3]_i$ increases from 200 to 600 mg L^{-1} . This is in agreement with Fathi et al. [39], who found that the heterogeneous precipitation rate, which was around 90% for 30 and 40 °F CaCO_3 solutions, reached 63% for 50 °F solution. The same observation can be made for Ben Amor et al. [38], who proved that when the water hardness increases from 20 to 50 °F, the $\%_{\text{hete}}$ decreases from 98 to 73%. Consequently, the adhesion of tartar on the cell walls is favored for low levels of calcium carbonate initially dissolved, and therefore for low nucleation thresholds. This can be due to the slow aggregation of ion pairs and clusters in low concentrated solutions, so the pre-nucleus remain at a small size for a longer time. Thus, it is more likely that they reach the surface and cling before they become large enough to not adhere to the cell wall.

3.2. Effect of Foreign Salts

3.2.1. Influence on the Nucleation Threshold

The most abundant salts found in natural waters are MgCl_2 , Na_2SO_4 and MgSO_4 . Their effect on the nucleation process of CaCO_3 will be investigated. The results of FCP tests obtained in PCCW- MgCl_2 , PCCW- Na_2SO_4 and PCCW- MgSO_4 solutions are compared to the results of PCCW solution. The pH and resistivity time curves are represented in Figures 5 and 6.

As shown in Table 2, the prenucleation time t_{prenuc} varies from 12 to 60 min as a function of the solution composition. During this time, the resistivity remains invariable, corresponding to the prenucleation threshold frontier. As expected, the increase of Mg^{2+} and SO_4^{2-} ions concentrations highly delays the nucleation time for both ionic strengths (Table 2). Any precipitation time obtained in the presence of foreign ions was more than the 46 min precipitation time of CaCO_3 in a PCCW solution. The MgSO_4 ion greatly delayed the precipitation of CaCO_3 compared to Mg^{2+} and SO_4^{2-} ions. Indeed, t_{prec} increased from 46 to 214 min when MgSO_4 concentration increased from 0 (IS_0) to 828 (IS_2) mg L^{-1} . As to Mg^{2+} and SO_4^{2-} , they increased the precipitation time from 46 min (PCCW) to only 102 and 64 min, respectively. Moreover, the ion pairs' formation (t_{prenuc}) and aggregation (t_{prec}) times were remarkably affected by the addition of each foreign ion. Indeed, the duration of the stable nuclei formation ($\Delta t = t_{\text{prec}} - t_{\text{prenuc}}$) was extended after the addition of these

ions to a PCCW solution. At the same ionic strength (IS_2), magnesium had more of an influence on the formation of $CaCO_3$ stable nuclei than sulfate since Δt was equivalent to 74 and 40 min for Mg^{2+} and SO_4^{2-} ions, respectively.

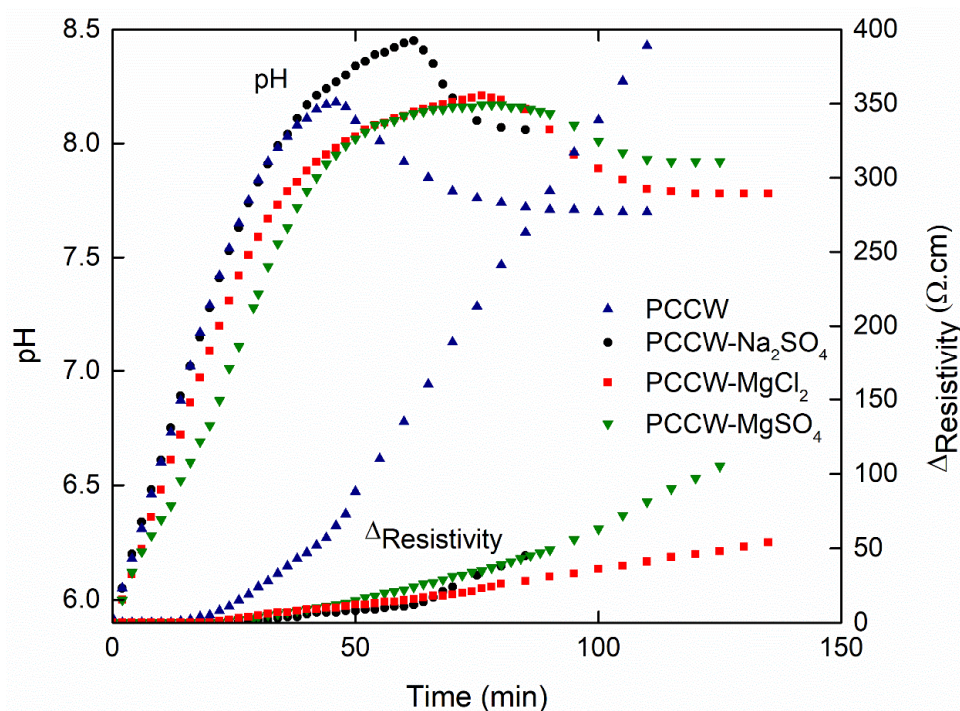


Figure 5. pH and $\Delta_{Resistivity}$ vs. time curves as a function of the added salt for IS_0 and IS_1 .

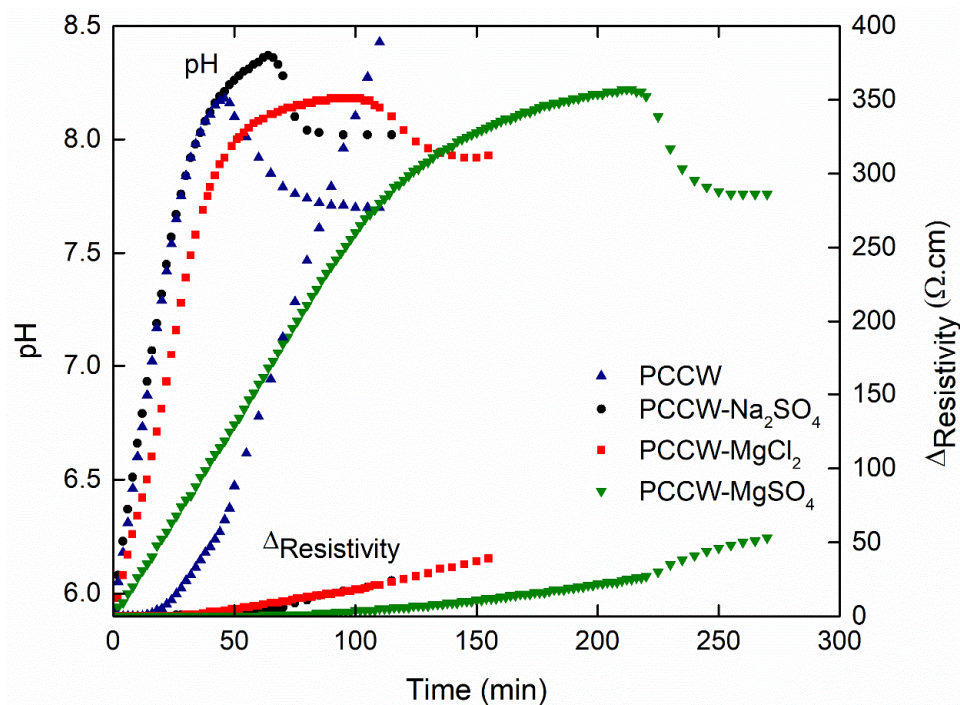


Figure 6. pH and $\Delta_{Resistivity}$ vs. time curves as a function of the added salt for IS_0 and IS_2 .

Table 2. FCP tests results by varying the added salt amount.

IS (mol L ⁻¹)	Solution	t _{prenuc} (min)	Ω _{prenuc}	t _{prec} (min)	Ω _{prec}	τ _{prec} (%)	% _{hete}
IS ₀ = 0.012	PCCW	12	1.7	46	48	45	45
IS ₁ = 0.024	PCCW-Na ₂ SO ₄	20	5.0	62	74	27	77
	PCCW-MgCl ₂	20	3.2	76	43	40	80
	PCCW-MgSO ₄	22	1.7	80	35	36	72
IS ₂ = 0.036	PCCW-Na ₂ SO ₄	24	8.7	64	55	26	72
	PCCW-MgCl ₂	28	4.4	102	35	38	79
	PCCW-MgSO ₄	60	1.6	214	33	35	71

Furthermore, Table 2 shows that the supersaturation coefficient values of the prenucleation threshold Ω_{prenuc} were very low and varied from 1 to 9. By contrast, the precipitation threshold was reached at high Ω_{prec} , especially after adding Na₂SO₄ to the PCCW solution. In fact, at the same ionic strength IS₁, SO₄²⁻ ion created a large supersaturation coefficient, which reached up to 1.55 times higher than the PCCW test (reference), while Mg²⁺ ion created a small supersaturation coefficient, which was 0.9 times lesser than that of PCCW. By combining these two ions to obtain MgSO₄, Ω_{prec} went down to 0.7 times less than that of PCCW. Consequently, sulfate ion had more of an impact on the pH of prenucleation and precipitation. As for magnesium ion, it influenced the nucleation time. Thus, the presence of magnesium and sulfate ions affected the nucleation and growth in different ways. Indeed, according to Waly et al. [40], two mechanisms can occur in the presence of magnesium and sulfate ions individually or together. The first mechanism involved is complexation, affecting the activity coefficients of calcium and carbonate ions by decreasing the total present ions for precipitation. The second implicated mechanism is inhibition, where the formed nuclei are inhibited from growing more by blocking the active growth sites. Therefore, both ions can attach to the recently formed calcium carbonate nuclei, causing a decrease in the nuclei growth rate due to the reduction in the available sites for growth by the blockage of the growth steps [41]. The growth can be suppressed entirely if the presence of foreign ions is dominant compared to the presence of calcium and carbonate ions [42].

3.2.2. Influence on the Surface Scaling

The effect of foreign ions on CaCO₃ formation has been investigated systematically in this paper, including aspects of kinetics, thermodynamics and behaviors. However, their influence on scale surface deposition has not yet been studied. For this, the total precipitation rate and the heterogeneous precipitation percentage are calculated using the weight method [38] in the absence and presence of foreign ions. As illustrated by Table 2, the total precipitation rate τ_{prec} decreases as the ionic strength increases. Indeed, τ_{prec} decreases for IS₁ by 5% for magnesium, 18% for sulfate and 9% for the two combined ions (MgSO₄) compared to the PCCW solution test. Moreover, τ_{prec} is practically invariant by increasing the ionic strength for each salt. Furthermore, in the presence of magnesium or sulfate ions or combined magnesium sulfate ions, more than 70% of the CaCO₃ precipitates are formed on the different surfaces in contact with water (cell-wall and probes) for both ionic strengths, whereas this heterogeneous percentage does not exceed 45% for pure calco-carbonic water. Subsequently, the introduction of one of these two ions, or both at once, leads to an increase in the precipitation on the walls for both ionic strengths studied. At the macroscopic scale, it would seem that both magnesium and sulfate ions, although presenting opposite charges, have the same effect on the orientation of CaCO₃ precipitation to the heterogeneous precipitation, regardless of their modes of action in solution. However, in the study of Chen et al. [43], it was proved that Mg²⁺ ions apparently inhibit both CaCO₃ bulk precipitation, regarded as a homogenous process, and CaCO₃ surface deposition, regarded as a heterogeneous process. It is known that Mg will bond with water and form a

complex at room temperature. This complex prohibits the nucleation and growth of calcite structure carbonate [44].

3.2.3. Influence on the Solid Precipitate Microstructure

The effect of foreign salts addition on the solid precipitate was studied. At the end of each FCP experiment, the precipitate obtained was characterized using the X-ray diffraction analyses. Figures 7–9 present, respectively, the XRD patterns of the precipitate obtained in the absence and presence of MgCl_2 , Na_2SO_4 and MgSO_4 for IS_1 and IS_2 . CaCO_3 precipitated in the PCCW is mainly vaterite, with a little fraction of calcite. The formation of these calcite crystals is inhibited when Mg^{2+} ions (from IS_1) and SO_4^{2-} ions are separately added (Figures 7 and 8). Nevertheless, the presence of Mg^{2+} promotes the aragonite (Figure 7), while SO_4^{2-} has no effect and vaterite remains the main CaCO_3 polymorphous (Figure 8). The action mode of magnesium ions can be by (i) the substitution of calcium ions, or (ii) the insertion in or (iii) adsorption on the CaCO_3 lattice [45]. If substitution or insertion leads to magnesian calcite, the adsorption at the earlier stage of nucleation and growth affects the CaCO_3 crystalline structure, which is the most probable action mode for our case. Indeed, the interactions between Mg and CaCO_3 nuclei are strong because they are improved by electrostatic interactions [46]. Moreover, Mg^{2+} competes with Ca^{2+} due to having the same charge, which favors the magnesium adsorption on the surface of calcite and vaterite [47]. The amount of Mg^{2+} being adsorbed onto CaCO_3 crystal active growth sites can be influenced by the precipitation rate and the local solution chemistry [22]. In the presence of MgSO_4 at IS_1 , the vaterite is completely transformed into aragonite (Figure 9) as for the precipitate obtained in MgCl_2 -solution (Figure 7). This confirms the role of magnesium ions in favoring the aragonite instead of vaterite. However, at such IS and in the presence of SO_4^{2-} , Mg^{2+} ions could not inhibit the crystallization of the calcite form (Figure 9). By increasing the ionic strength (IS_2) in the case of MgSO_4 , calcite is gradually inhibited.

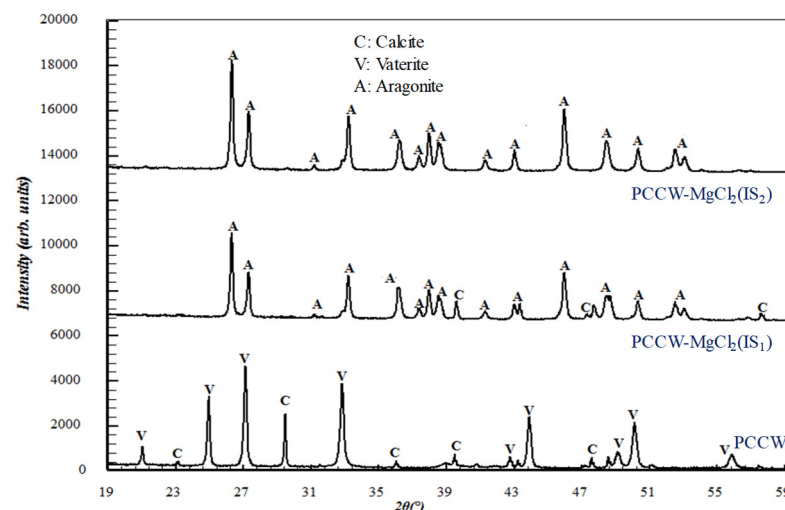


Figure 7. XRD patterns of the precipitate formed in the presence of MgCl_2 by varying IS .

3.3. Effect of Antiscalant

3.3.1. Influence on the Nucleation Threshold

Calcium carbonate scale deposits in natural water installations are a stimulating issue, mainly by obstructing the water flow. The formation of such undesirable deposits can be inhibited by the addition of antiscalants such as organic sodium salt of polyacrylate (RPI) and inorganic sodium tripolyphosphate (STPP). The results of FCP tests obtained in PCCW-RPI and PCCW-STPP solutions were compared to the results of the PCCW solution.

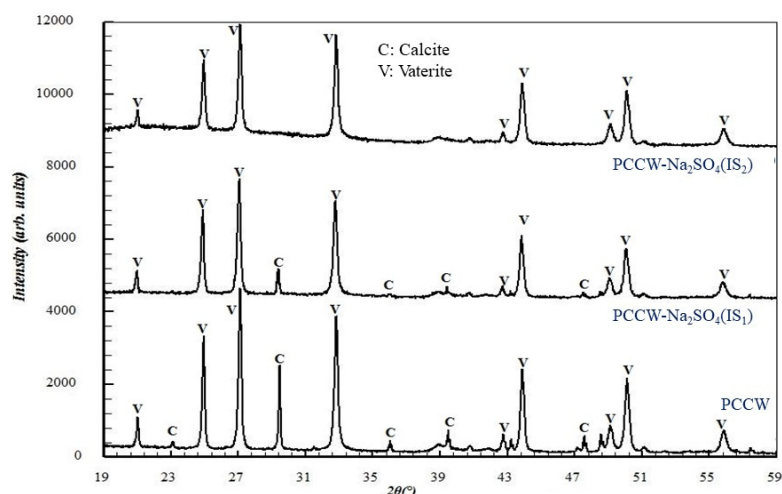


Figure 8. XRD patterns of the precipitate formed in the presence of Na_2SO_4 by varying IS.

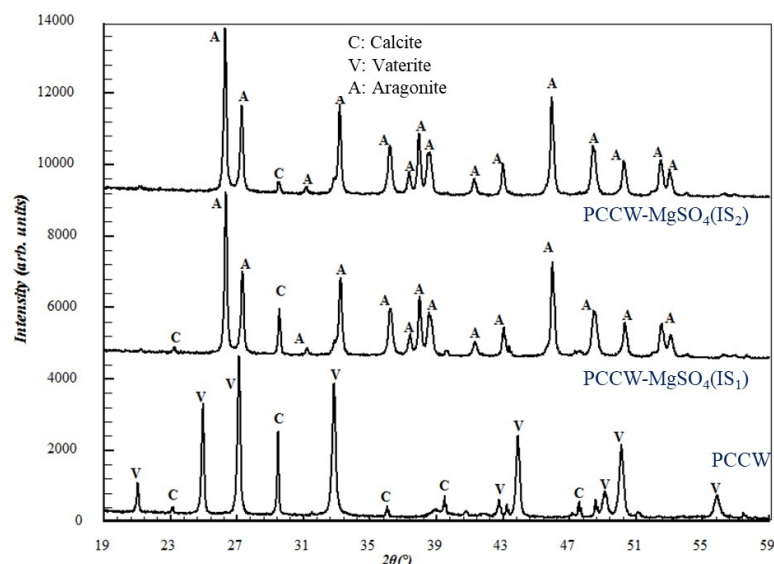


Figure 9. XRD patterns of the precipitate formed in the presence of MgSO_4 by varying IS.

Figures 10 and 11 report the temporal evolution of pH and $\Delta_{\text{Resistivity}}$ as a function of RPI and STPP antiscalants amount. They show that the presence of both antiscalants RPI and STPP significantly influences the kinetics of the nucleation process. Indeed, t_{prenuc} increased from 12 min for PCCW to 20 min in the presence of 4 ppm RPI and 0.8 ppm STPP, as seen in Table 3. During this time, the resistivity remained invariable corresponding to the prenucleation threshold limit. In addition, the increase of the antiscalant amount added to PCCW led to a higher precipitation time. In addition, STPP greatly delayed the precipitation of CaCO_3 compared to RPI. In fact, t_{prec} increased from 46 to 210 min and to 365 min for 4 ppm RPI and 0.8 ppm STPP, respectively. Furthermore, the duration of the stable nuclei formation ($\Delta t = t_{\text{prec}} - t_{\text{prenuc}}$) was longer as the antiscalant amount was larger. Therefore, the distinction between the prenucleation and precipitation thresholds became easier. Moreover, the prenucleation threshold was always attained at Ω_{prenuc} values less than 7. Conversely, the precipitation threshold was reached at very high Ω_{prec} , especially after adding STPP to PCCW solution, which went up to 353 at 0.8 ppm. Consequently, both antiscalants affected the kinetics and thermodynamics of calcium carbonate prenucleation and precipitation with different manners.

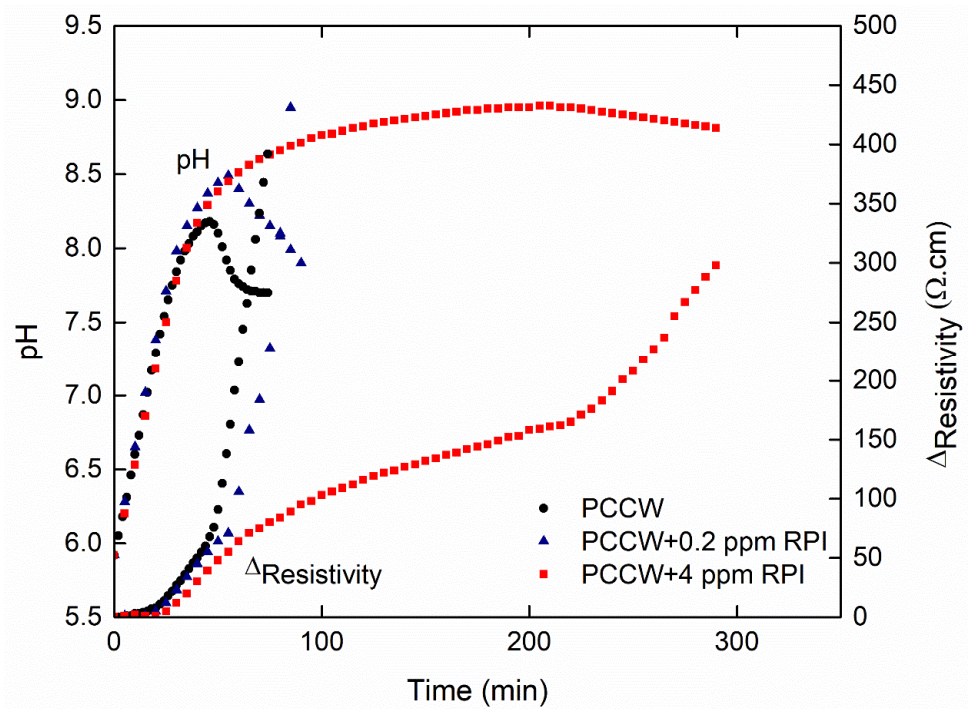


Figure 10. pH and $\Delta_{\text{Resistivity}}$ vs. time curves as a function of RPI amount.

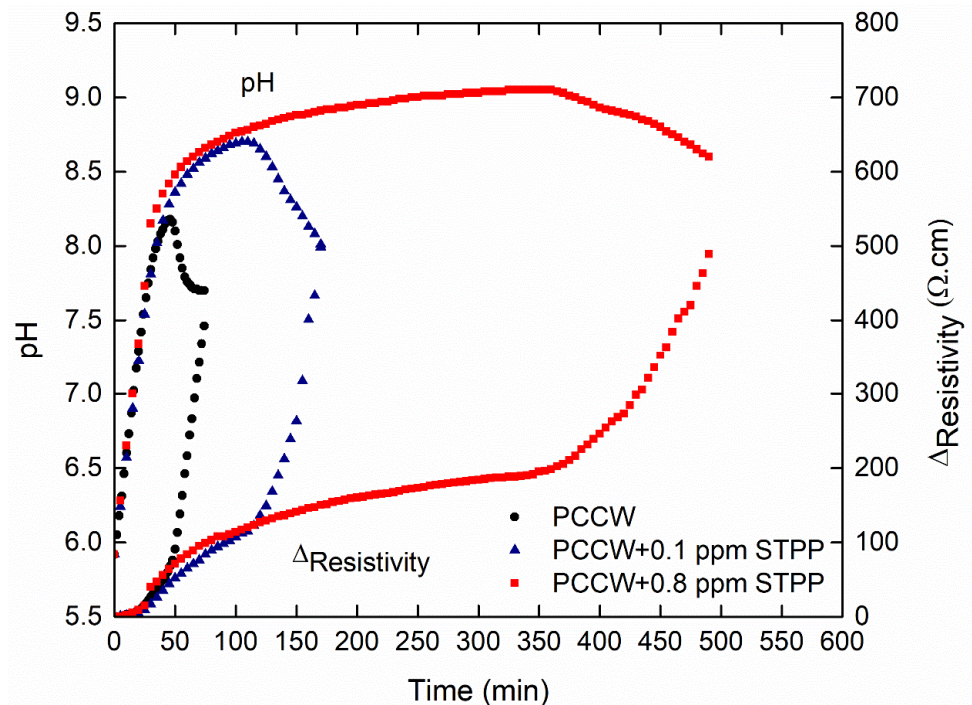


Figure 11. pH and $\Delta_{\text{Resistivity}}$ vs. time curves as a function of STPP amount.

3.3.2. Influence on the Surface Scaling

The influence of the two antiscalants on scale surface deposition was studied by calculating the total precipitation rate and the heterogeneous precipitation percentage using the weight method. As seen in Table 3, after the addition of each antiscalant, the total precipitation rate τ_{prec} decreased remarkably from 45% for PCCW to 29% and 33% in the presence of RPI (4 ppm) and STPP (0.8 ppm), respectively. Moreover, for the same antiscalant, τ_{prec} decreased by increasing its amount added to PCCW. Furthermore, both antiscalants greatly affected the scale adherence to the cell wall and probes. Indeed, $\%_{\text{hete}}$ increased from 45%

for PCCW to 79% and to 70% after adding 4 ppm of RPI and 0.8 ppm of STPP, respectively. Despite RPI being organic and STPP being inorganic antiscalants, they both favorably promote precipitation on the cell wall detrimentally to the bulk solution scaling.

Table 3. FCP test results by varying the antiscalant amount.

Solution	t_{prenuc} (min)	Ω_{prenuc}	t_{prec} (min)	Ω_{prec}	τ_{prec}	% _{hete}
PCCW	12	1.7	46	48	45	45
PCCW-RPI (0.2 ppm)	15	3	55	97	34	74
PCCW-RPI (4 ppm)	20	5	210	286	29	79
PCCW-STPP (0.1 ppm)	15	2.5	110	157	37	66
PCCW-STPP (0.8 ppm)	20	7	365	353	33	70

3.3.3. Influence on the Solid Precipitate Microstructure

The X-ray diffraction patterns of the precipitate formed in the presence of RPI and STPP are presented in Figures 12 and 13. The patterns of deposit scale obtained in PCCW reveal the formation of calcite with majority vaterite. After the addition of 4 ppm RPI, the crystallization was orientated towards the formation of calcite and to the complete inhibition of vaterite. In the presence of 0.8 ppm STPP, the phases formed remained vaterite and calcite, with the appearance of a new aragonite phase. Consequently, the two antiscalants acted on the CaCO_3 precipitation in different ways. XRD characterizations proved that the presence of antiscalant can affect the morphology and the crystal shape of calcium carbonate [48].

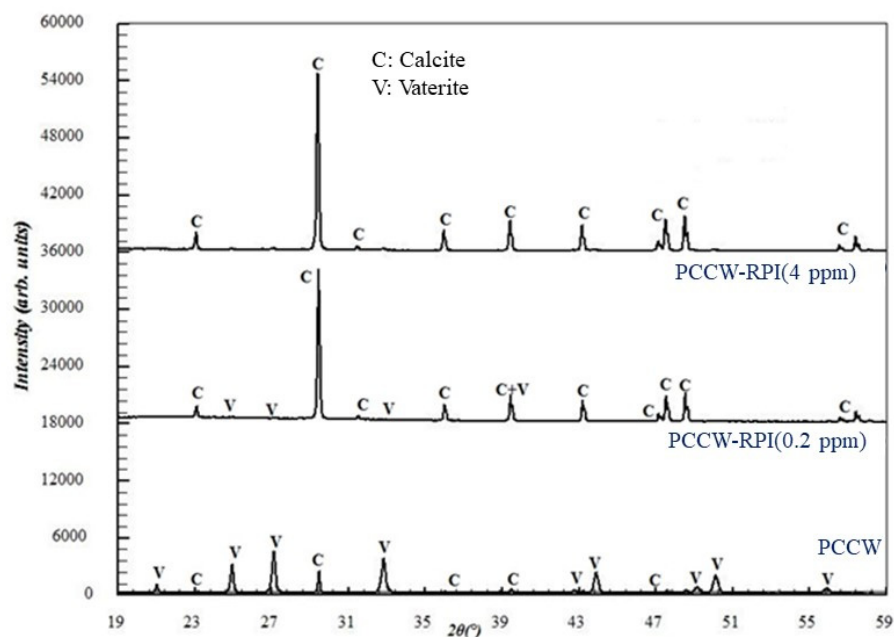


Figure 12. XRD patterns of the precipitate formed in the presence of RPI.

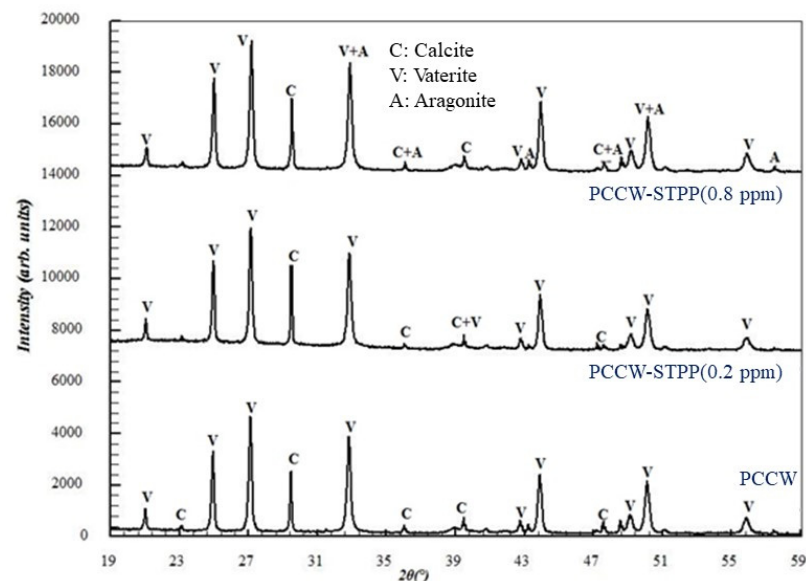


Figure 13. XRD patterns of the precipitate formed in the presence of STPP.

4. Conclusions

Chemical additives play a significant role in several stages of the formation and transformation of CaCO_3 crystals. In the present paper, the fast controlled precipitation method was used to study the influence of chemical additives on the CaCO_3 crystallization process. The additives employed were three foreign salts (MgCl_2 , Na_2SO_4 and MgSO_4) and two antiscalants (sodium polyacrylate and sodium-tripolyphosphate). The results showed that the nucleation time was retarded after the addition of each foreign salt, regardless of its ionic strength value. The MgSO_4 ion greatly delayed the precipitation of CaCO_3 compared to Mg^{2+} and SO_4^{2-} ions. Moreover, the sulfate ion had more impact on the pH of prenucleation and precipitation. As for magnesium ion, it influenced the nucleation time. Thus, the presence of magnesium and sulfate ions affected nucleation and growth through different ways. At the macroscopic scale, it would seem that both magnesium and sulfate ions, although presenting opposite charges, had the same effect on the orientation of CaCO_3 precipitation to the heterogeneous precipitation, regardless of their modes of action in solution. Furthermore, both antiscalants RPI and STPP had a great effect on the crystallization kinetic by greatly delaying the precipitation time. Indeed, the prenucleation stage duration ($\Delta t = t_{\text{prec}} - t_{\text{prenuc}}$) was longer when the antiscalant concentration was larger. Therefore, the distinction between the prenucleation and precipitation thresholds became easier. In addition, the presence of each antiscalant affected the precipitation threshold remarkably, leading to a large variation in the supersaturation coefficient. In addition, the chemical inhibition favorably promoted precipitation on the cell wall, detrimental to the bulk solution scaling. Finally, the X-ray diffraction patterns of deposit scale formed in the absence and presence of each chemical additive revealed the formation of different crystal forms of calcium carbonate, which were calcite, vaterite and aragonite.

Author Contributions: Conceptualization, R.H. and M.M.T.; methodology, R.H. and M.M.T.; software, R.H.; validation, R.H. and M.M.T.; formal analysis, R.H. and M.M.T.; investigation, R.H.; resources, R.H. and M.M.T.; data curation, R.H.; writing—original draft preparation, R.H.; writing—review and editing, R.H. and M.M.T.; visualization, R.H.; supervision, R.H. and M.M.T.; project administration, R.H. and M.M.T.; funding acquisition, R.H. and M.M.T. All authors have read and agreed to the published version of the manuscript.

Funding: This research was funded by the Deputyship for Research and Innovation, Ministry of Education in Saudi Arabia, Project number (IF2/PSAU/2022/01/21605).

Institutional Review Board Statement: Not applicable.

Informed Consent Statement: Not applicable.

Data Availability Statement: Data are available on reasonable request.

Acknowledgments: The authors extend their appreciation to the Deputyship for Research and Innovation, Ministry of Education in Saudi Arabia for funding this research work through the Project number (IF2/PSAU/2022/01/21605).

Conflicts of Interest: The authors declare no conflict of interest.

References

1. Lu, J.; Ruan, S.; Liu, Y.; Wang, T.; Zeng, Q.; Yan, D. Morphological characteristics of calcium carbonate crystallization in CO₂ pre-cured aerated concrete. *RSC Adv.* **2022**, *12*, 14610–14620. [[CrossRef](#)] [[PubMed](#)]
2. Feng, Z.; Yang, T.; Dong, S.; Wu, T.; Jin, W.; Wu, Z.; Wang, B.; Liang, T.; Cao, L.; Yu, L. Industrially synthesized biosafe vaterite hollow CaCO₃ for controllable delivery of anticancer drugs. *Mater. Today Chem.* **2022**, *24*, 100917. [[CrossRef](#)]
3. Lu, H.; Huang, Y.-C.; Hunger, J.; Gebauer, D.; Cölfen, H.; Bonn, M. Role of Water in CaCO₃ Biomineralization. *J. Am. Chem. Soc.* **2021**, *143*, 1758–1762. [[CrossRef](#)] [[PubMed](#)]
4. Kontrec, J.; Tomašić, N.; Mlinarić, N.M.; Kralj, D.; Džakula, B.N. Effect of pH and Type of Stirring on the Spontaneous Precipitation of CaCO₃ at Identical Initial Supersaturation, Ionic Strength and a(Ca²⁺)/a(CO₃²⁻) Ratio. *Crystals* **2021**, *11*, 1075. [[CrossRef](#)]
5. Dobberschütz, S.; Nielsen, M.R.; Sand, K.K.; Civioc, R.; Bovet, N.; Stipp, S.L.S.; Andersson, M.P. The mechanisms of crystal growth inhibition by organic and inorganic inhibitors. *Nat. Commun.* **2018**, *9*, 1578. [[CrossRef](#)]
6. Lázár, A.; Molnár, Z.; Demény, A.; Kótai, L.; Trif, L.; Béres, K.A.; Bódis, E.; Bortel, G.; Aradi, L.E.; Karlik, M.; et al. Insights into the amorphous calcium carbonate (ACC) → ikaite → calcite transformations. *CrystEngComm* **2023**, *25*, 738–750. [[CrossRef](#)]
7. Dong, L.; Xu, Y.-J.; Sui, C.; Zhao, Y.; Mao, L.-B.; Gebauer, D.; Rosenberg, R.; Avaro, J.; Wu, Y.-D.; Gao, H.-L.; et al. Highly hydrated paramagnetic amorphous calcium carbonate nanoclusters as an MRI contrast agent. *Nat. Commun.* **2022**, *13*, 5088. [[CrossRef](#)]
8. Raffaella, D.; Paolo, R.; Julian, D.G.; David, Q.; Denis, G. Stable prenucleation mineral clusters are liquid-like ionic polymers. *Nat. Commun.* **2011**, *2*, 590.
9. Gebauer, D.; Völkel, A.; Cölfen, H. Stable prenucleation calcium carbonate clusters. *Science* **2008**, *322*, 1819–1822. [[CrossRef](#)]
10. Ostwald, W. Studies on formation and transformation of solid materials (Studien über die bildung und umwandlung fester körper). *Z. Phys. Chem.* **1897**, *22*, 289–330. [[CrossRef](#)]
11. Hamdi, R.; Tlili, M.M. Influence of foreign salts on the CaCO₃ pre-nucleation stage: Application of the conductometric method. *CrystEngComm* **2022**, *24*, 3256–3267. [[CrossRef](#)]
12. Wolf, S.L.P.; Jähme, K.; Gebauer, D. Synergy of Mg²⁺ and poly(aspartic acid) in additive-controlled calcium carbonate precipitation. *CrystEngComm* **2015**, *17*, 6857–6862. [[CrossRef](#)]
13. Song, R.-Q.; Cölfen, H. Additive controlled crystallization. *CrystEngComm* **2011**, *13*, 1249–1276. [[CrossRef](#)]
14. Raj, K.S.; Devi, M.N.; Palanisamy, K.; Subramanian, V.K. Individual and synergetic effect of EDTA and NTA on polymorphism and morphology of CaCO₃ crystallization process in presence of barium. *J. Solid State Chem.* **2021**, *302*, 122026.
15. Sancho-Tomás, M.; Fermani, S.; Durán-Olivencia, M.A.; Otálora, F.; Gómez-Morales, J.; Falini, G.; García-Ruiz, J.M. Influence of Charged Polypeptides on Nucleation and Growth of CaCO₃ Evaluated by Counterdiffusion Experiments. *Cryst. Growth Des.* **2013**, *13*, 3884–3891. [[CrossRef](#)]
16. Ihli, J.; Kim, Y.-Y.; Noel, E.H.; Meldrum, F.C. The Effect of Additives on Amorphous Calcium Carbonate (ACC): Janus Behavior in Solution and the Solid State. *Adv. Funct. Mater.* **2013**, *23*, 1575–1585. [[CrossRef](#)]
17. Xiang, L.; Xiang, Y.; Wang, Z.G.; Jin, Y. Influence of chemical additives on the formation of super-fine calcium carbonate. *Powder Technol.* **2002**, *126*, 129–133. [[CrossRef](#)]
18. Davis, K.J.; Dove, P.M.; De Yoreo, J.J. The Role of Mg²⁺ as an Impurity in Calcite Growth. *Science* **2000**, *290*, 1134–1137. [[CrossRef](#)]
19. Loste, E.; Wilson, R.M.; Seshadri, R.; Meldrum, F.C. The role of magnesium in stabilising amorphous calcium carbonate and controlling calcite morphologies. *J. Cryst. Growth* **2003**, *254*, 206–218. [[CrossRef](#)]
20. Chong, T.H.; Sheikholeslami, R. Thermodynamics and kinetics for mixed calcium carbonate and calcium sulfate precipitation. *Chem. Eng. Sci.* **2001**, *56*, 5391–5400. [[CrossRef](#)]
21. Chen, T.; Neville, A.; Yuan, M. Assessing the effect of Mg²⁺ on CaCO₃ scale formation–bulk precipitation and surface deposition. *J. Cryst. Growth* **2005**, *275*, e1341–e1347. [[CrossRef](#)]
22. Zhang, Y.; Dawe, R.A. Influence of Mg²⁺ on the kinetics of calcite precipitation and calcite crystal morphology. *Chem. Geol.* **2000**, *163*, 129–138. [[CrossRef](#)]
23. Niedermayr, A.; Köhler, S.J.; Dietzel, M. Impacts of aqueous carbonate accumulation rate, magnesium and polyaspartic acid on calcium carbonate formation (6–40 °C). *Chem. Geol.* **2013**, *340*, 105–120. [[CrossRef](#)]
24. Blue, C.R.; Giuffrè, A.; Mergelsberg, S.; Han, N.; De Yoreo, J.J.; Dove, P.M. Chemical and physical controls on the transformation of amorphous calcium carbonate into crystalline CaCO₃ polymorphs. *Geochim. Cosmochim. Acta* **2017**, *196*, 179–196. [[CrossRef](#)]
25. Rodríguez-Blanco, J.D.; Shaw, S.; Bots, P.; Roncal-Herrero, T.; Benning, L.G. The role of Mg in the crystallization of monohydrocalcite. *Geochim. Cosmochim. Acta* **2014**, *127*, 204–220. [[CrossRef](#)]

26. Zhang, A.; Xie, H.; Liu, N.; Chen, B.-L.; Ping, H.; Fu, Z.-Y.; Su, B.-L. Crystallization of calcium carbonate under the influences of casein and magnesium ions. *RSC Adv.* **2016**, *6*, 110362–110366. [[CrossRef](#)]
27. Nielsen, M.R.; Sand, K.K.; Rodriguez-Blanco, J.D.; Bovet, N.; Generosi, J.; Dalby, K.N.; Stipp, S.L.S. Inhibition of Calcite Growth: Combined Effects of Mg^{2+} and SO_4^{2-} . *Cryst. Growth Des.* **2016**, *16*, 6199–6207. [[CrossRef](#)]
28. Sheikholeslami, R.; Ong, H.W.K. Kinetics and thermodynamics of calcium carbonate and calcium sulfate at salinities up to 1.5 M. *Desalination* **2003**, *157*, 217–234. [[CrossRef](#)]
29. Tang, Y.; Zhang, F.; Cao, Z.; Jing, W.; Chen, Y. Crystallization of $CaCO_3$ in the presence of sulfate and additives: Experimental and molecular dynamics simulation studies. *J. Colloid Interface Sci.* **2012**, *377*, 430–437. [[CrossRef](#)]
30. Hamdi, R.; Tlili, M.M. Investigation of scale inhibitors effect on calcium carbonate nucleation process. *Desalination Water Treat.* **2019**, *160*, 14–22. [[CrossRef](#)]
31. Jain, T.; Sanchez, E.; Owens-Bennett, E.; Trussell, R.; Walker, S.; Liu, H. Impacts of antiscalants on the formation of calcium solids: Implication on scaling potential of desalination concentrate. *Environ. Sci. Water Res. Technol.* **2019**, *5*, 1285–1294. [[CrossRef](#)]
32. Bai, S.; Naren, G.; Nakano, M.; Okaue, Y.; Yokoyama, T. Effect of polysilicic acid on the precipitation of calcium carbonate. *Colloids Surf. A Physicochem. Eng. Asp.* **2014**, *445*, 54–58. [[CrossRef](#)]
33. Chhim, N.; Haddad, E.; Neveux, T.; Bouteleux, C.; Teychené, S.; Biscans, B. Performance of green antiscalants and their mixtures in controlled calcium carbonate precipitation conditions reproducing industrial cooling circuits. *Water Res.* **2020**, *186*, 116334. [[CrossRef](#)] [[PubMed](#)]
34. Eichinger, S.; Boch, R.; Leis, A.; Baldermann, A.; Domberger, G.; Schwab, C.; Dietzel, M. Green inhibitors reduce unwanted calcium carbonate precipitation: Implications for technical settings. *Water Res.* **2022**, *208*, 117850. [[CrossRef](#)]
35. Gauthier, G.; Chao, Y.; Horner, O.; Alos-Ramos, O.; Hui, F.; Lédion, J.; Perrot, H. Application of the Fast Controlled Precipitation method to assess the scale-forming ability of raw river waters. *Desalination* **2012**, *299*, 89–95. [[CrossRef](#)]
36. Lédion, J.; François, B.; Vienne, J. Characterization of the scaling properties of water by fast controlled precipitation test. *Eur. J. Water Qual.* **1997**, *28*, 15–35. [[CrossRef](#)]
37. Rosset, R.; Sok, P.; Poindessous, G.; Amor, M.B.; Walha, K. Caractérisation de la compacité des dépôts de carbonate de calcium d'eaux géothermales du Sud tunisien par impédancemétrie. *Comptes Rendus L'académie Sci. Ser. IIC Chem.* **1998**, *1*, 751–759. [[CrossRef](#)]
38. Amor, M.B.; Zgolli, D.; Tlili, M.M.; Manzola, A.S. Influence of water hardness, substrate nature and temperature on heterogeneous calcium carbonate nucleation. *Desalination* **2004**, *166*, 79–84. [[CrossRef](#)]
39. Fathi, A.; Mohamed, T.; Claude, G.; Maurin, G.; Mohamed, B.A. Effect of a magnetic water treatment on homogeneous and heterogeneous precipitation of calcium carbonate. *Water Res.* **2006**, *40*, 1941–1950. [[CrossRef](#)]
40. Waly, T.; Kennedy, M.D.; Witkamp, G.-J.; Amy, G.; Schippers, J.C. The role of inorganic ions in the calcium carbonate scaling of seawater reverse osmosis systems. *Desalination* **2012**, *284*, 279–287. [[CrossRef](#)]
41. Mullin, J.W. *Crystallization*; Butterworth-Heinemann: Oxford, UK, 2001.
42. Söhnel, O.; Garside, J.H. *Precipitation: Basic Principles and Industrial Applications*; Butterworth-Heinemann: Oxford, UK, 1992.
43. Chen, T.; Neville, A.; Yuan, M. Influence of on formation—Bulk precipitation and surface deposition. *Chem. Eng. Sci.* **2006**, *61*, 5318–5327. [[CrossRef](#)]
44. Fang, Y.; Zhang, F.; Farfan, G.A.; Xu, H. Low-Temperature Synthesis of Disordered Dolomite and High-Magnesium Calcite in Ethanol–Water Solutions: The Solvation Effect and Implications. *ACS Omega* **2022**, *7*, 281–292. [[CrossRef](#)]
45. Tlili, M.M.; Amor, M.B.; Gabrielli, C.; Joiret, S.; Maurin, G.; Rousseau, P. Study of Electrochemical Deposition of $CaCO_3$ by In Situ Raman Spectroscopy: II. Influence of the Solution Composition. *J. Electrochem. Soc.* **2003**, *150*, C485–C493. [[CrossRef](#)]
46. Zahid, A. *Mineral Scale Formation and Inhibition*; Plenum Press: New York, NY, USA, 1995.
47. Compton, R.G.; Brown, C.A. The Inhibition of Calcite Dissolution/Precipitation: Mg^{2+} Cations. *J. Colloid Interface Sci.* **1994**, *165*, 445–449. [[CrossRef](#)]
48. Sheng, K.; Ge, H.; Huang, X.; Zhang, Y.; Song, Y.; Ge, F.; Zhao, Y.; Meng, X. Formation and Inhibition of Calcium Carbonate Crystals under Cathodic Polarization Conditions. *Crystals* **2020**, *10*, 275. [[CrossRef](#)]

Disclaimer/Publisher's Note: The statements, opinions and data contained in all publications are solely those of the individual author(s) and contributor(s) and not of MDPI and/or the editor(s). MDPI and/or the editor(s) disclaim responsibility for any injury to people or property resulting from any ideas, methods, instructions or products referred to in the content.